Title: ELECTRON PHOTON VERIFICATION
CALCULATIONS USING MCNP4B

CONF-980403--

RECEIVED
JUL 01 1998
OSTI

Author(s): David P. Gierga, XCI
Kenneth J. Adams, XCI

Submitted to: 1998 Radiation Protection and Shielding
Division Topical Conference Nashville,
TN 4/19-23/98

MASTER

# Los Alamos
NATIONAL LABORATORY

# DISCLAIMER

# DISCLAIMER

**Portions of this document may be illegible electronic image products. Images are produced from the best available original document.**

# Electron Photon Verification Calculations Using MCNP4B

David P. Gierga and Kenneth J. Adams
Los Alamos National Laboratory
Los Alamos, NM

## Abstract

MCNP4B was released in February 1997 with significant enhancements to electron/photon transport methods. These enhancements have been verified against a wide range of published electron/photon experiments, spanning high energy bremsstrahlung production to electron transmission and reflection. Three sets of bremsstrahlung experiments were simulated. The first verification calculations for bremsstrahlung production used the experimental results of Faddegon for 15 MeV electrons incident on lead, aluminum, and beryllium targets. The calculated integrated bremsstrahlung yields, the bremsstrahlung energy spectra, and the mean energy of the bremsstrahlung beam were compared with experiment. The impact of several MCNP tally options and physics parameters was explored in detail. The second was the experiment of O'Dell which measured the bremsstrahlung spectra from 10 and 20.9 MeV electrons incident on a gold/tungsten target. The final set was a comparison of relative experimental spectra with calculated results for 9.66 MeV electrons incident on tungsten based on the experiment of Starfelt and Koch. The transmission experiments of Ebert were also studied, including comparisons of transmission coefficients for 10.2 MeV electrons incident on carbon, silver, and uranium foils. The agreement between experiment and simulation was usually within two standard deviations of the experimental and calculational errors.

## 1. Introduction

MCNP (Monte Carlo N-Particle) is a three dimensional, fully coupled neutron-photon-electron Monte Carlo transport code. MCNP version 4B[1], released in February 1997, included significant enhancements to the electron-photon transport methods. These included improvements in secondary particle production algorithms and the mitigation of electron substep artifacts, as well as improved stopping powers and energy loss parameter. The purpose of this study was to compare the simulation results of MCNP4B with several experiments in the literature. This paper describes the bremsstrahlung production and electron transmission calculations. Further information is available in (ref LA report?).

## 2. Description

### 2.1 Bremsstrahlung Verification Calculations

Several thick-target bremsstrahlung calculations were performed. The targets are "thick" in that their thickness is greater than an electron range; the targets are thin to photons. Previous studies on these data have been performed using EGS[2,5], ITS[3], and MCNP4A[4]. MCNP4B simulations of three sets of experiments are described. They are the absolute thick-target bremsstrahlung measurements of Faddegon et al.[6,7] and O'Dell et al.[8], as well as the relative bremsstrahlung measurements of Starfelt and Koch[9].

The bremsstrahlung simulations included both cell and detector photon tallies. Detector and cell flux tallies are calculated in fundamentally different ways. The cell tally for flux is a track length estimate, in which the time integrated flux is estimated by the summing $WT_l/V$, where $W$ is the particle weight, $T_l$ is the track length of the particle in the cell, and $V$ is the cell volume. Conversely, a detector tally is a deterministic estimate of the flux at a point in space, or in the case of a ring detector tally, at a point sampled from some location on a ring. The detector flux is calculated from[1]

$$\Phi(\mathbf{r}, E, \mu) = \frac{Wp(\mu)e^{-\lambda}}{2\pi R^2},$$ (1)

where $2p(\mu)$ is the probability density function at $\mu$, the cosine of the angle between the particle trajectory and the direction to the detector; $R$ is the distance from the source or collision event to the detector; and

$$\lambda = \int_0^R \Sigma_t(s) ds.$$ (2)

which is the total number of mean free paths integrated over the trajectory from the source or collision event to the detector, $\Sigma_t$ is the total macroscopic cross section.

The exponential term of Eq. (2) accounts for the attenuation between the present event and the detector point, and a $1/4\pi R^2$ term accounts for the solid angle effect. The $p(\mu)$ term accounts for the probability of scattering toward the detector instead of the direction selected in the random walk. Each contribution to the detector can be thought of as transporting a "pseudoparticle" to the detector.

### 2.1.1 Faddegon *et al.* Experiment

The most detailed set of the three bremsstrahlung calculations described in this paper were the MCNP simulations of the experiments of Faddegon *et al.*[6,7]. These experiments provided bremsstrahlung spectra and integrated yields from thick targets of Be, Al, and Pb at angles of 0°, 1°, 2°, 4°, 10°, 30°, 60°, and 90° relative to the beam axis for electrons of 15 MeV incident energy. The spectra are absolute in the sense that they are in units of photons per incident electron.

The electron beam passed through a thin Ti exit window (0.013 cm) and a Si beam monitoring detector (0.01 cm) prior to impinging on the target chamber. The targets were Pb (9.13 g/cm² thick, 17.95 g/cm² radius), Al (9.74 g/cm² thick, 9.81 g/cm² radius), and Be (11.67 g/cm² thick, 6.72 g/cm² radius) cylinders. The targets are thick for electrons, but not for photons. The targets were surrounded by a stainless steel target chamber, except for the 30°, 60°, and 90° measurements. There was an additional Al exit window downstream of the target. The photons then passed through a Pb collimator prior to being collected in a NaI detector. Both the experiment and simulations used a low energy cutoff of 145 keV.

The Monte Carlo simulation was designed to match the experiment as faithfully as possible. The work of DeMarco[4], who performed a similar study using MCNP4A, was used extensively as a reference. The Al target exit window, side walls of the stainless steel target chamber, and Pb collimator were not included in the simulation since the published experimental results are corrected for these factors. The simulations were done in a vacuum, since the experimental data is also corrected for attenuation in air. The target dimensions corresponded exactly to the published values. The thicknesses for the Ti exit window and Si beam monitory system were taken from the published values, although the radial dimensions were estimated. Further uncertainty is introduced in modeling the stainless steel entrance window. In the MCNP model, the stainless steel was defined as 18% (weight fraction) chromium, 8% nickel, and 76% iron. This model was based on typical 304 stainless steel, neglecting the trace impurities.

The bremsstrahlung yields were tallied using cell flux and detector flux tallies. The spectral data over individual energy bins were tallied, although the primary item of interest was the bremsstrahlung yield integrated over all energies. The tallies were multiplied by the square of the source to detector distance (SDD) to convert the tally units from photons per cm² to photons per steradian. The SDD of 300 cm is defined from the upstream surface of the target. The cell tallies were based on the union of two cones and two spheres, which forms an annular spherical region. An angular range of 0.5° and a radial thickness of 1 mm were used. Ring detectors were defined according to the SDD and a ring radius which reproduces the desired angle. Since the geometry is cylindrically symmetric, ring detectors were used rather than point detectors for maximum efficiency. The MCNP default settings were used for this set of calculations, as well as for all other calculations presented in this paper, unless otherwise noted.

### 2.1.2 Starfelt and Koch Experiment

Starfelt and Koch[9] have also measured thick target bremsstrahlung spectra. They report photon spectra for 9.66 MeV electrons incident on a tungsten target for 0° and 12°. They used an electron beam from a 50 MeV betatron which passed through a system of Lucite collimators in order to minimize the angular spread of the beam. The electron current in the target was not measured so the spectra are not absolute. The beam was focused on the bremsstrahlung target by an iron-core magnetic lens. Targets were mounted on aluminum rings 1 mm thick with 52 mm inside diameters. The tungsten target was 5.8 $g/cm^2$ thick. The bremsstrahlung photons pass through an aluminum window, cadmium filter, and lead collimator before impinging on a NaI(Tl) spectrometer.

Since the photon spectra were corrected for collimator effects and photon absorption between target and spectrometer, the only material included in the simulation was the target. Electron and photon cutoff energies were set to 0.4 MeV. Cell and detector tallies were positioned at 0° and 12° using the same method as described in the previous section. The cell tallies had an angular range of 0.7°, which is consistent with the experimental setup. To reconcile the differences between the relative experimental results and the absolute MCNP calculations the experimental data were normalized to the simulation at the first (lowest) energy bin.

### 2.1.3 O'Dell et al. Experiment

O'Dell et al.[8] measured the thick target bremsstrahlung spectra for 5.3 to 20.9 MeV electrons incident on a gold-tungsten target. The bremsstrahlung target was 0.49 $g/cm^2$ of tungsten followed by 0.245 $g/cm^2$ of gold. The spectra were measured using a technique based on deuteron photodisintegration. This method is limited to measuring photon energies above 3 MeV[6]. The electrons were incident on the bremsstrahlung target, and the resulting photons interact with a secondary $D_2O$ target, which provides a source of photoneutrons. The neutrons produced above the $D(\gamma,n)p$ reaction threshold of 2.23 MeV were analyzed using time-of-flight techniques. This gives absolute bremsstrahlung spectra in units of photons per MeV per steradian per incident electron.

The bremsstrahlung target was modeled as a thin cylinder of tungsten followed by a thin cylinder of gold. Simulations using 10.0 and 20.9 MeV incident electrons were done. The secondary target was modeled with dimensions of 1.25 x 0.25 and 0.5 x 0.25 in. for the 10.0 and 20.9 measurements, respectively. The photon spectrum was tallied over the entire face of the cell. This is important since the bremsstrahlung yield is fairly sensitive to angle, especially near 0°[10]. Electron and photon low energy cutoffs were set to 4.0 MeV, which mirror the published experimental result. Only the electron beam and bremsstrahlung target were modeled, with the photons being tallied over the face of the $D_2O$ target.

### 2.2 Electron Transmission and Backscatter

Several electron transmission and backscatter comparisons were also done. Ebert et al.[11] give a tremendous amount of data for 4.0 to 12.0 MeV monoenergetic electrons incident on a variety of solid targets. In this study, a few of the experimental transmission and backscatter experiments have been simulated using MCNP4B.

In this experiment, the electron beam, generated by a linac, had an energy spread of about 1%. The beam passed through two copper collimators, chosen as a compromise between a low-Z, low density material which would produce a large low energy secondary electron background, and a high Z, high density material which would produce a high bremsstrahlung background. The maximum beam diameter allowed by the collimators was 0.6 cm at the target.

The target chamber contained x-ray shielding, an insulated target holder, two large Faraday cups, and a carbon beam stop in addition to the collimator assembly. The Faraday cups were used to collect the transmitted and backscattered electrons. Bias rings, set to -500 V, were mounted in the Faraday cups to minimize the very low energy secondary electron current. The targets ranged in thickness from about 0.03 to 6.0 $g/cm^2$. The targets were either 2.0 or 8.0 cm in diameter. The larger targets ranged in linear thickness from 0.6 to 3.2 cm. The target dimensions were chosen such that the target radius was greater than the sum of the beam radius and the maximum electron range. This configuration will minimize electron escape through the target sides, and approximate a semi-infinite slab geometry.

The experimental geometry was greatly simplified for the MCNP simulations. Only the target was explicitly modeled. The transmission and backscatter coefficients were calculated using particle current tallies at the target faces. This is much simpler than modeling the Faraday cup geometry, and ensures that there are no tally losses from solid angle effects. The current tallies were divided into two $\cos(\theta)$ bins, where $\theta$ is defined relative to the positive surface normal. The transmission coefficient was calculated by using a $\theta$ range of 0° to 90°, while the backscatter

coefficient used a θ range of 90° to 180°. The simulations were done in coupled electron/photon mode, and used the default cutoffs of 1 keV.

## 3. Results

### 3.1 Faddegon Comparison

The integrated bremsstrahlung yield for a Pb target is presented in Figure 1. Simulations for angles between 0° and 10° include the stainless steel entrance window, while angles greater than 10° had no stainless steel window. This is consistent with the experiment.
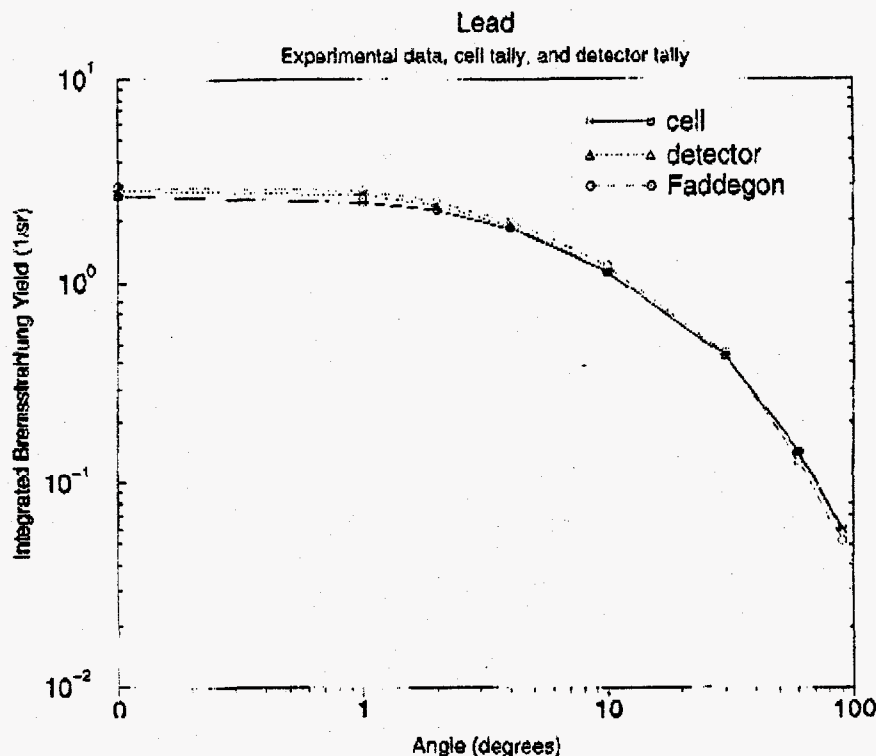


**Figure 1: Integrated Bremsstrahlung Yield vs Angle for Pb.**

Figure 1 shows that the discrepancies between experiment and simulation are greatest for the forward directed angles and for 90°. It is interesting to note that the detector tally seems to track the experiment better than the cell tally, even though more detailed physics is used for the cell tally for electron photon problems. When the same physics models are used, however, the cell and detector tallies become identical. The largest difference between experiment and simulation is 16% at 90° for cell tallies, and 13% at 90° for detector tallies. The error bars for the 0° and 90° simulations were generally the largest, because of the low intensity at 90° and small the solid angle at 0°.

The detailed energy spectra were also compared. Figure 2 shows experimental and simulation results for the bremsstrahlung energy spectra for aluminum. These plots compare the default MCNP cell tally with experimental data at 10°. The simulations show excellent overall agreement for each material. These results show that MCNP can accurately calculate both the integrated bremsstrahlung yields as well as the detailed photon energy spectra.
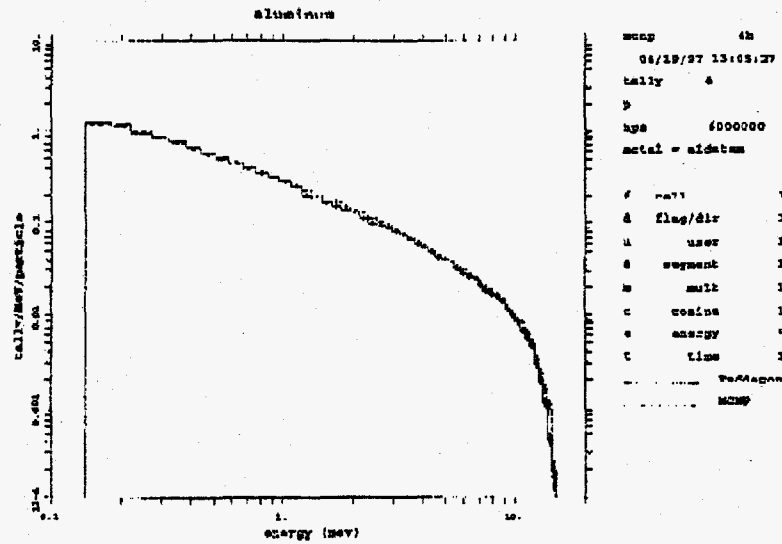
**Figure 2: Comparison of experimental and MCNP cell tally bremsstrahlung spectra for aluminum at 10°.**

## 3.2 Starfelt and Koch Comparison

Figure 3 shows the 0° bremsstrahlung spectra as a function of photon energy. The experimental and MCNP spectral shapes show good agreement for both angles, and in fact agree within statistical uncertainty. The spectra agree particularly well for lower photon energies, which correspond to the highest photon yields. Error bars are not shown for the experimental data, but Starfelt and Koch estimate the uncertainties to range from about 3-4% at 1 MeV to 11-17% at 9 MeV. The experimental errors become quite large for photon energies above 95% of the incident electron energy.
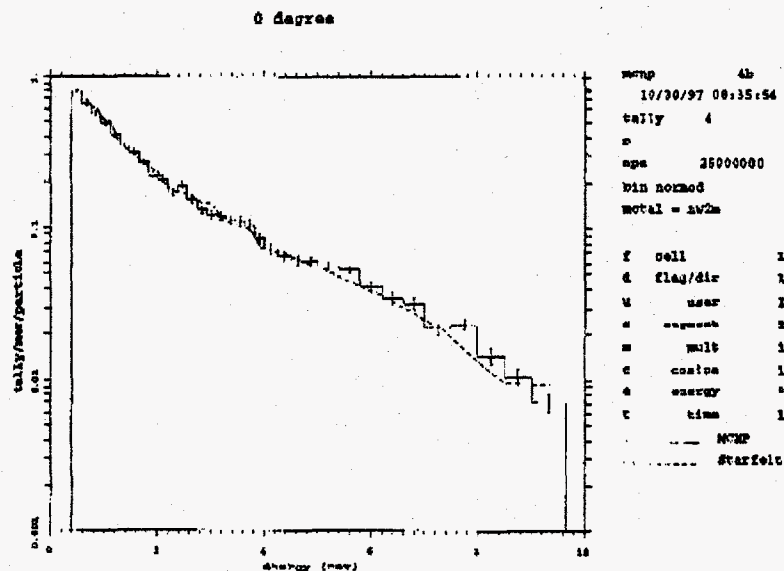


**Figure 3: Experimental and calculated bremsstrahlung spectrum at 0° for 9.66 MeV electrons incident on tungsten**

## 3.3 O'Dell Comparison

Calculated and experimental bremsstrahlung spectra are shown in Figure 4 for 20.9 MeV electrons incident on a gold/tungsten target. Error bars for the experimental data are based on O'Dell's estimate that the errors range from 5 to 10%, except at higher photon energies where poor counting statistics further increase the experimental error. There is good overall agreement between calculation and experiment at both energies. All of the points agree within experimental error. There also appear to be some minor discontinuities in the MCNP simulations. These are most likely statistical in nature, and are not a reflection of the cross section data. This can be verified by running the simulation for more histories.

Table 1 gives the integrated bremsstrahlung yields for the Au/W target at 10.0 and 20.9 MeV. The results for O'Dell were obtained by integrating the published spectra, while the MCNP result was automatically obtained from the cell tally. The results show that MCNP agrees with experiment to within 5%.
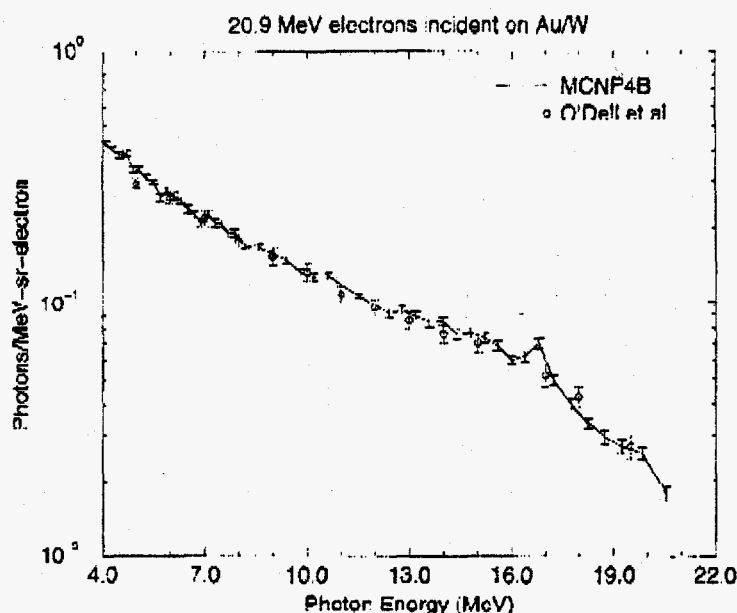


Figure 4: Bremsstrahlung Energy Spectrum, 20.9 MeV electrons incident on Au/W.

Table 3.1: Integrated Yields for Au/W for O'Dell

| Energy (MeV) | O'Dell (1/sr) | MCNP (1/sr) |
|---|---|---|
| 10.0 | 0.1826 (23.6,7.5[a]) | 0.1949 (0.93) |
| 20.9 | 2.0929 (29.0,7.5) | 2.1956 (0.48) |

[a] first number is propagated percent error, second is percent error in each experimental data point

## 3.4 Ebert Results

Transmission coefficients for 10.2 MeV electrons incident on Ag foils of varying thicknesses are presented in

Figure 5. The experimental results and simulation results using MCNP4B default settings are shown. The simulations agree with experiment with varying degrees of success. The experimental uncertainties are estimated at 2%; Ebert *et al*. only give a errors for transmission coefficients between 0.3 and 0.8.

The silver simulations agree with experiment to the greatest degree. The maximum deviation between the default simulation and experiment is 17%, while most of the transmission coefficients agree within 10%. For the range of transmission coefficients that experimental uncertainties are published, the simulation and experiment agree within statistics. For carbon (not shown), the default MCNP simulations disagree with experiment by as much as 90% for the last few data points, although the transmission coefficients for thicknesses less than 3.5 g/cm$^2$ differ within 10%. The experimental uncertainties in the transmission coefficients for very thick targets may be quite large, which may help account for these discrepancies. For uranium (not shown), default MCNP agrees with experiment within 5-15%.
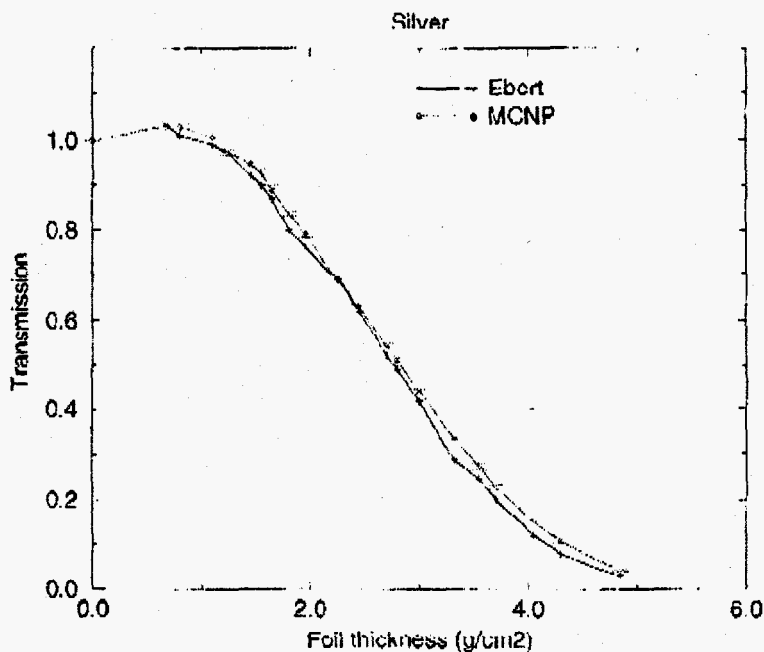


**Figure 5: Comparison of transmission coefficients for 10.2 MeV electrons incident on Ag foils**

# 4. Conclusions

MCNP4B was verified against a wide range of electron/photon experiments including high energy bremsstrahlung production and electron transmission and reflection. The bremsstrahlung spectral shape and mean energy compared well across three benchmark experiments. The energy integrated yields agreed within about 10% for cell tallies and 5% for detector tallies when comparing to the experiments of Faddegon *et al*., except for a few points near 0° and 90°. The cell tally energy integrated yields for O'Dell *et al*., however, agreed to within 5% of the experiment, and were slightly higher than the experimental results. MCNP also showed excellent agreement with the bremsstrahlung spectra of Starfelt and Koch. The calculations of electron transmission based on the experiments of Ebert *et al*. compare within 5-15% for silver and uranium, but there are highly significant deviations for carbon. The calculations in this study have shown that MCNP achieves excellent agreement with a wide range of experiments

# 5. References

1. J.F. Briesmeister, "MCNP - A general Monte Carlo N-Particle transport code, version 4B," Los Alamos National Laboratory Report, LA-12625-M (1997).

2. W.R. Nelson, H. Hirayama, D.W.O. Rogers. "The EGS4 code system," SLAC-Report-265, Stanford Linear Accelerator Center (Dec. 1985).

3. J. A. Halbleib, R. P. Kensek, T. A. Mehlhorn, G. D. Valdez, S. M. Seltzer, and M. J. Berger, "ITS Version 3.0: The Integrated TIGER Series of Coupled Electron/Photon Monte Carlo Transport Codes," Sandia National Laboratories report SAND91-1634 (March 1992).

4. J.J. DeMarco, T.D. Soldberg, R.E. Wallace, J.B. Smathers, "A verification of the Monte Carlo code MCNP for thick target bremsstrahlung calculations," *Med. Phys.* **22**, p. 11-16, (1995).

5. B.A. Faddegon, D.W.O Rogers, "Comparisons of thick-target bremsstrahlung calculations by EGS4/PRESTA and ITS version 2.1," *Nuc. Inst. Meth.* A **327**, p. 556-565 (1993).

6. B.A. Faddegon, C.K. Ross, D.W.O. Rogers, "Forward-directed bremsstrahlung of 10- to 30-MeV electrons incident on thick targets of Al and Pb," *Med. Phys.* **17**, p. 773 785, (1990).

7. B.A. Faddegon, C.K. Ross, D.W.O. Rogers, "Angular distribution of bremsstrahlung from 15-MeV electrons incident on thick targets of Be, Al, and Pb," *Med. Phys.* **18**, p. 727-739 (1991).

8. A.A. O'Dell, C.W. Sandifer, R.B. Knowlen, W.D. George, "Measurement of Absolute thick-target Bremsstrahlung Spectra," *Nuc. Inst. Meth.* **61**, p. 340-346 (1968).

9. N. Starfelt and H.W. Koch, "Differential Cross-Section Measurements of Thin-target Bremsstrahlung Produced by 2.7 to 9.7 MeV Electrons," *Phys. Rev.* **102**, p.1598-1612 (1956).

10. M.J. Berger and S.M. Seltzer, "Bremsstrahlung and Photoneutrons from Thick Tungsten and Tantalum Targets," *Phys. Rev.* C **2**, p. 621-631, (1970).

11. P.J. Ebert, A.F. Lauzon, E.M. Lent, "Transmission and Backscattering of 4.0- to 12.0-MeV Electrons," *Phys. Rev.* **183**, p.422-430 (1969).